

## Novel Lead Configurations for Robust Bio-Impedance Acquisition

Joel Ironstone, MIEEE  
Z-Tech (Canada) Inc.

Milan Graovac, P. Eng  
Department of Electrical and  
Computer Engineering,  
University of Toronto

James Martens  
Department of  
Mathematics, University of  
Waterloo

Martin Rozee, MIEEE  
Z-Tech (Canada) Inc.

K.C. Smith, P. Eng. LFIEEE  
Professor Emeritus, University  
of Toronto

### Abstract

*This paper describes a diagnostic medical instrument that has undergone a multi-centre 6500-patient clinical trial to evaluate its effectiveness as a replacement for screening X-Ray mammography. The device uses a single bipolar current source multiplexed to two 32-element electrode arrays. The multiplexer allows three novel lead configurations to be measured in addition to the common tetrapolar configuration used in many impedance-acquisition systems. These additional configurations allow pre-testing of electrode contacts, post-testing assessment of measurement fidelity and correction for the effect of shunt-capacitive pathways. The results of the clinical trial show that the device can be operated reliably by individuals with only one day of specialized training and that the device can distinguish between normal and diseased breasts.*

### 1. Introduction

When tissue undergoes cancerous change, there is a corresponding change in measured electrical properties [1]. Clinical results identify bioelectric-impedance analysis as a possible method of non-invasively detecting breast cancer [2]. In previous clinical studies, diagnostic sensitivity and specificity were too low for the technique to be used effectively as a screening tool. The authors of the study attributed the high rate of false positives to poor electrode-to-skin contact and air bubbles in the electrode gel [3]. In this paper, three novel lead configurations are described that allow for a significant reduction in the likelihood of measurement error from such sources. This is accomplished by providing useful feedback to the operator before and after data acquisition, and using additional measurements to correct for systematic errors.

Feedback on the state of electrode contacts provided to the operator prior to scanning allows them to secure lifting contacts or replace faulty electrode arrays.

### 2. System Description



Figure 1. Azura BreastScan™ System

The system described in this paper, and shown in Figure 1, is the Azura BreastScan™ System [7]. A block diagram of the system is shown in Figure 2. It consists of four primary components: Laptop Computer, Main Unit, Front-End Module (FEM), and two bilaterally symmetric SuperStellate™ electrode arrays.

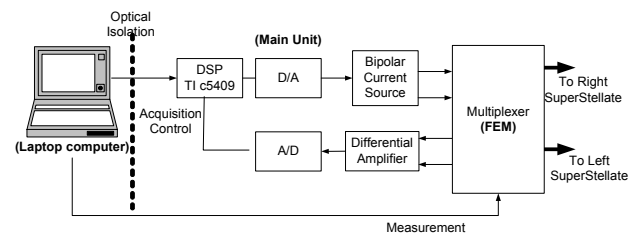


Figure 2. Azura BreastScan™ Block Diagram

The interface to the patient is through two bilaterally symmetric electrode arrays (SuperStellates™) which are self-adhesive and pre-gelled monolithic components. Each electrode array is centred about the nipple, and has 'petals' extending to the breast boundary. Each petal contains either one or two electrode pairs. Figure 3 shows a left electrode array attached to a patient.



**Figure 3.** SuperStellate™ Electrode Array applied to a patient.

Each electrode pair consists of a current-injection electrode and a voltage-measurement electrode in close proximity, separated by non-conductive adhesive foam. The electrodes are single-use disposable items manufactured with biocompatible materials.

The Laptop controls measurement acquisition by communicating with the multiplexer in the FEM to select measurements. Under instruction from the Laptop, the DSP in the Main Unit executes an impedance acquisition. The DSP operates a D/A circuit which controls a constant sinusoidal current source whose frequency and burst duration are programmable. The current source is multiplexed to connect two current-injection leads on one of the two 32-element electrode arrays. The multiplexer also selects two voltage measurement leads whose voltages are differentially amplified and returned to the Main Unit for digitization in the A/D.

### 3. System Operational Overview

The described system can operate at specified frequencies between 10 kHz and 125 kHz. A full test, called an Azura BreastScan™, includes 528 measurements at five frequencies for each of the left and right breasts (a total of 5280 measurements) and is completed in less than 3 minutes. Measurement acquisition proceeds from lowest to highest frequency. An algorithm compares the measurements acquired on the left and right breasts to determine an impedance-asymmetry score which is correlated with neoplastic change. Based on this score, further diagnostic tests can be recommended.

The 528 measurements per frequency and breast are of four types as follows: 48 *Contact*, 120 *Vsame*, 240 *Impedance Matrix*, and 120 *Bipolar*. Figure 4 shows a cross-sectional schematic of these four measurement configurations as applied to three current-voltage electrode pairs [8].

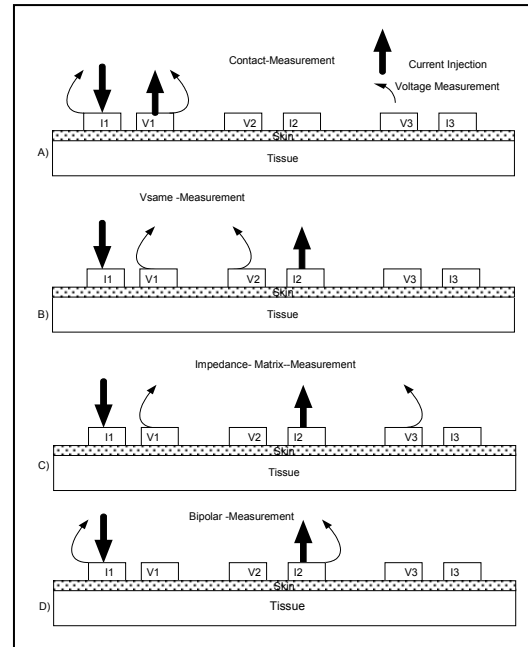


**Figure 4.** Four Azura BreastScan™ Measurement Configurations

Each of these measurement configurations is described below:

**A) Contact:** Involves a single electrode pair, where voltage is measured between the electrodes used for current-injection: one of which is characterized as being a current-injection electrode and the other as a voltage-measurement electrode.

**B) Vsame:** Involves two electrode pairs where voltage is measured between the voltage-measurement electrodes associated with the active current-injection electrodes.

**C) Impedance Matrix:** Involves three electrode pairs where voltage-measurement is between one of the pairs associated with current-injection and a separate other.

**D) Bipolar:** Involves two pairs, where voltage is measured between the current-injection electrodes.

The Vsame measurements are used for computing an impedance-asymmetry score; the primary output of the instrument. The other measurement types are used to provide the operator with feedback concerning the consistency of the acquired data, and to provide a post-acquisition calibration. These auxiliary functions will be described in detail in the following sections.

#### 4. Contact Measurements and the Real-Time Electrode-Contact Display

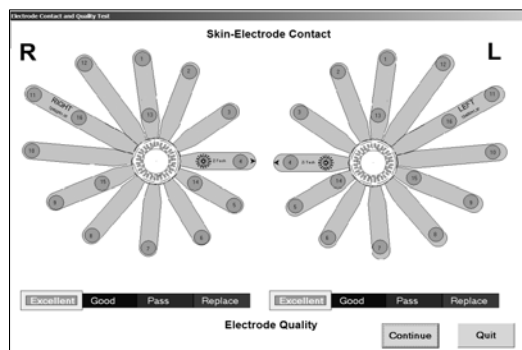


Figure 5. The Skin-Electrode Contact Screen

Before each impedance data acquisition, the operator is presented with the Skin-Electrode Contact Screen depicted in Figure 5. The screen displays a schematic of the patient-right and patient-left electrode arrays. The colour of the circles representing each electrode pair indicates whether that pair is making sufficient contact with the skin. A blue circle indicates adequate contact, and a red circle indicates a problem. Each contact is numbered to allow the operator to identify them on the patient. The quality indicator at the bottom displays the average impedance magnitude of all contacts on that electrode array. Contact measurements as shown in Figure 4 A) are used to generate this display. While this display is visible, the device is constantly cycling through the sixteen electrode pairs on each breast, acquiring magnitude and phase data. As each measurement takes less than 20 ms to complete, the set of 32 (16 for each breast) contact measurements is acquired and updated on the screen in less than 0.5 seconds.

The skin has a large capacitive [4] component in the Contact configuration. This component is especially sensitive to changes in skin contact, making phase angle a good indicator of adequacy of contact. The magnitude of the contact impedance is determined primarily by the quality of the electrode gel, particularly its hydration [4]. If the gel in an electrode array dries out due to improper storage or handling, impedance magnitude will increase. The average magnitude of contact impedance measurements for an electrode array is summarized by the electrode quality indicator [11].

By acquiring a set of extra measurements, and displaying them in real time on an easily interpretable interface, electrode application and electrode quality problems can be corrected before data acquisition begins. The effect of any corrective action is immediately visible

to the operator, who can continue the test with a single mouse-click when all contacts are secured.

#### 5. Impedance Matrix Measurements and Data-Consistency Calculation and Display

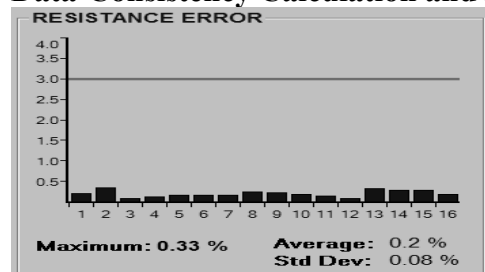


Figure 6. Resistance-Error Display

The graph shown in Figure 6 is displayed after the complete set of measurements is acquired. This display shows the error in the resistive component of impedance measurements associated with each electrode. This error is calculated by comparing the two independent sets of data acquired for each breast at each frequency. The  $V_{same}$  results can be shown to be theoretically computable from the Impedance Matrix results by application of superposition and Kirchoff's voltage law [9].

#### 6. Bipolar Measurements and Shunt-Current Compensation

Azura BreastScan™ System is designed with a single bipolar current source multiplexed to its stimulation-and-measurement electrodes. Although very-low-capacitance multiplexers (MAX4051ACPE) are used to switch the signals, the large series impedance of human skin, which can exceed 15 kΩ at 17kHz [5], will cause significant error in impedance measurement, by forcing current through pre-electrode shunt-capacitive pathways. Earlier instruments were restricted to frequencies below 50 kHz to minimize effects related to shunt capacitance [6].

Figure 7 shows a schematic of a simplified model of the effect of shunt capacitance and large skin resistances on measured results.

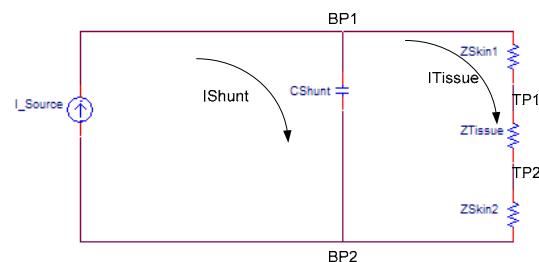
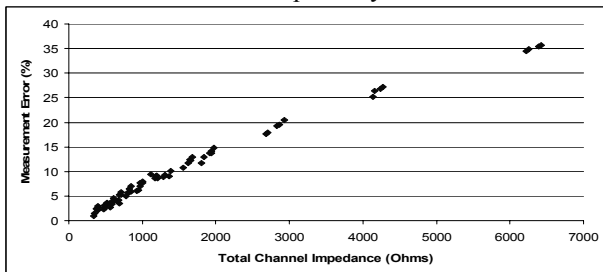


Figure 7. Schematic showing the dependence of shunt-current on contact impedance.

As the skin contact impedances, ( $Z_{Skin1}$  and  $Z_{Skin2}$ ), increase, the current, ( $I_{Shunt}$ ), going through the shunt capacitance, ( $C_{Shunt}$ ) increases, with the result that current, ( $I_{Tissue}$ ) through the tissue impedance ( $Z_{Tissue}$ ), and the voltage  $V(TP1)-V(TP2)$  across  $Z_{Tissue}$  decreases. This effect is predictable, and by measuring the voltage on the current-injection leads, one can estimate the impedance that the entire current channel sees, and therefore calculate the current through the capacitor  $C_{Shunt}$ . Bipolar measurements, as described in Figure 4 D), and measured between nodes BP1 and BP2, provide the ability to do this. As the bipolar measured impedance increases, the measurement error associated with shunt pathways increases.



**Figure 8.** Plot of  $V_{same}$  Measurement Errors vs. Total Channel Impedance at 50 kHz

Figure 8 shows a plot of the error of measured data as the series impedance of the skin increases at 50 kHz. By using Bipolar measurements to identify where on this curve a particular tetrapolar  $V_{same}$  measurement is located, a correction factor can be obtained. When this correction factor is applied, measurement error is reduced from a continually increasing function to less than  $\pm 2\%$  over the entire range of possible skin impedances (Figure 9) [10].

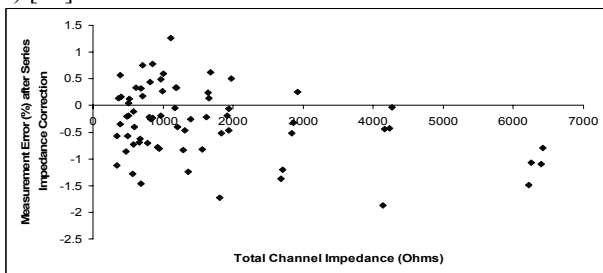


**Figure 9.** Plot of  $V_{same}$  Measurement Errors vs. Total Channel Impedance at 50 kHz, after application of Correction Factors

## 7. Results

In the clinical trial, 5580 of 6494 subjects had successful scans, representing an 86% test success rate. More than 20% of these successful tests began with initially poor contacts which were secured during the electrode-contact screening process. Therefore, the electrode contact screen contributed to a substantial increase in test success rate.

Of the women successfully measured in the study, 358 had a biopsy-verified breast cancer. The impedance-asymmetry score for women with verified breast cancer, with a mean of 210, was significantly higher than those without breast cancer with a mean of 45 ( $p$  value  $< 0.0001$ ).

## 7. Conclusion

By employing novel lead configurations, robust and clinically-viable impedance measurements can be obtained. Four different lead configurations were discussed that reduce the likelihood of measurement errors and correct those that persist. These usability innovations, combined with the use of a bilateral comparison, provide a reliable method for breast-cancer screening, one that was proven effective in this clinical trial.

## 8. Acknowledgements

The authors gratefully acknowledge Dr. Leslie Organ and Zoran Pavlovic for their invaluable contributions to this project, and Tim Xu, David Wang, Shing Fan, and Frank Zhang, for their continued work on this technology.

## 9. References

- [1] B. Børhe and B. Baldetop, "Impedance Spectra of tumour tissue in comparison with normal tissue; a possible clinical application for electrical impedance tomography," *Physiol. Meas.*, vol. 17, pp A105-A115, 1996
- [2] T.E. Kerner, K.D. Paulsen, A.H. Hartov, S.K. Soho, and S.P. Poplack, "Electrical Impedance Spectroscopy of the Breast: Clinical Imaging Results in 26 Subjects," *IEEE Trans. Med. Imag.*, vol 21, no 6. pp 638-645, 2002.
- [3] A. Malich, T. Fritsch, R. Anderson, T. Boegm, M.G. Freesmeyer, M. Fleck, and W.A. Kaiser, "Electrical Impedance Scanning for Classifying Suspicious Breast Lesions: First Results," *Eur. Radiol.*, vol. 10, No. 10, pp 1555-1561, 2000.
- [4] H. Tagami, "Hardware and Measuring Principle: Skin Conductance," *Bioengineering of the Skin: Water and the Stratum Corneum*, P. Elsner, E. Berardesca, H.I. Maibach, Ed. CRC Press, Boca Raton FL, 1994.
- [5] I. Nicander, P. Aberg, and S. Ollmar, "The use of different concentrations of betaine as a reducing irritation agent in soaps monitored visually and non-invasively," *Skin Res Technol*, vol. 9(1) 43-9. Feb 2003, pp 43-49.
- [6] V.A. Cherepenin, A.Y. Karpov, V.N. Kornienko, Y.S. Kultiasov, and M.B. Ochapkin, O.V. Trochanova, J.D. Meister, "Three-Dimensional EIT Imaging of Breast Tissues: System Design and Clinical Testing," *IEEE Trans. Biomed. Eng.*, vol. 21, no. 6, pp. 662-667, June 2002
- [7] L.W. Organ et al. "Electrical Impedance Method and Apparatus for detecting and Diagnosing Disease," US Patent #6,768,921
- [8] K.C. Smith, J. Ironstone, F. Zhang, "Bioimpedance measurement using controller-switched current injection and multiplexer selected electrode connection," US Patent #7,212,853
- [9] L.W. Organ, "Electrical impedance method and apparatus for detecting and diagnosing diseases," US Patent #6,122,544
- [10] K.C. Smith, J. Ironstone, "Eliminating interface artifact errors in bioimpedance measurements," United States Patent Application #20040181164
- [11] L.W. Organ, K.C. Smith, J. Ironstone, "Apparatus and method for determining adequacy of electrode-to-skin contact and electrode quality for bioelectrical measurements," United States Patent Application # 20040243018